Dopant electrical activity and majority-carrier mobility in B- and Sb-δ-doped Si thin films

H.-J. Gossmann and F. C. Unterwald
AT&T Bell Laboratories, Murray Hill, New Jersey 07974
(Received 9 November 1992)

The electrical characteristics of Si films grown by low-temperature molecular-beam epitaxy and doped with Sb or B in single or multiple δ-like doping profiles have been investigated. Two-dimensional concentrations ranging from $\approx 10^{13}$ cm^{-2} to 5×10^{14} cm^{-2} have been realized. For single doping spikes Hall measurements indicate an apparent reduction in electrical activity to about 50%. This is linked to the confinement of the carriers in the potential well of the doping spike. The reduced electrical activity is not due to growth imperfections. The effect of the confinement on the Hall measurements can be reduced in δ-doping superlattices, provided the distance between doping spikes is sufficiently small. For $N_{Sb}^{2D}=10^{13}$ cm^{-2} the mobility in a δ-doping superlattice drops exponentially as a function of inverse spike spacing until, at about 5 nm, a value close to the mobility in an equivalent, uniformly doped film ($N_{Sb}\approx 3\times10^{19}$ cm^{-3}) is reached. Carrier mobilities in δ-doped layers far exceed those of uniformly doped layers of equivalent concentration. Electron mobilities reach 400 cm^2/V s for a sheet concentration of 1×10^{13} cm^{-2} and are still at $\approx$40 cm^2/V s at $N_{Sb}^{2D}=5\times10^{14}$ cm^{-2}. For *p*-type doping these numbers are 180 and 20 cm^2/V s, respectively.

I. INTRODUCTION

One of the characteristic features of epitaxial growth techniques, such as molecular-beam epitaxy (MBE), is the prospect of controlling constituents and dopants in a thin film on an atomic scale, almost in an arbitrary fashion. Atomically abrupt transitions in composition, for example, from Si to Ge, or in the concentration of dopants, allow the demonstration of new physical phenomena.[1–3] The ultimate limit on the abruptness is a δ-function-like spike. This is referred to as "δ doping" if it is the dopant that is confined to the spike. Such two-dimensional (2D) doping sheets are integral parts of many semiconductor device concepts. Although δ doping was demonstrated in GaAs in 1985 (Ref. 4) its practical realization in Si was long retarded by the difficulty of introducing dopants into Si in a well controlled way during epitaxial growth. Recent advances in the understanding of epitaxial growth and the incorporation of dopants in Si have overcome these difficulties and opened a new field in Si materials and device research.[5] Presently, the fabrication of both *n*- and *p*-type δ-doped Si films has been demonstrated.[6–9] The smallest spatial extents, as measured by secondary-ion-mass spectrometry, have been reported for samples grown by low-temperature MBE (LT MBE), with a full width at half maximum of <2.7 nm for an Sb-doped spike and a leading edge slope of 0.94 nm/decade for a B profile.[10]

The small spatial extent of the dopant distribution in δ-doped layers may lead to extreme peak volume concentrations, exceeding the solid solubility by orders of magnitude. While this is desirable in certain device applications it is not obvious that the resulting material still has good electrical properties. Of further interest is the maximum electrically active sheet concentration. Here we report on a systematic study of electrical activity and carrier mobility in *n*(Sb)- and *p*(B)-δ-doped films. All structures were grown by LT MBE. Two-dimensional electrical concentrations up to 3×10^{14} cm^{-2} have been achieved. By investigating δ-doping superlattices (δ-DSL) we will show that the apparent reduction in electrical activity observed in films with a single doping spike is due to the confinement of the carriers in the potential well of the dopant. We will demonstrate that carrier mobilities in δ-doped layers far exceed those of uniformly doped layers of equivalent concentration.

II. EXPERIMENT

Growth and doping of Si thin films by LT MBE have been described extensively elsewhere.[5,10] Briefly, LT MBE is based on the realization that the traditional concept of an epitaxial temperature, separating the regime of epitaxial, single-crystalline growth of the film from the regime of amorphous growth, is not appropriate for the growth of Si.[11] Instead, Si always grows epitaxially on Si(100) until a certain thickness, h_{epi}, is reached, where growth turns amorphous. This thickness falls off exponentially with decreasing temperature following an Arrhenius relation.[12] Growth of epitaxial layers of thickness $m\times h_{epi}$, $m=1,2,\ldots$, is accomplished by interrupting growth and executing rapid thermal anneal (RTA) cycles to temperatures $T_{RTA}>500$ °C for 100 s every h_{epi}.[11] Since segregation of dopants can be suppressed kinetically at growth temperatures below $\approx$450 °C, LT MBE makes the growth of arbitrarily complex doping profiles by thermal coevaporative doping feasible.

All samples were grown in a custom-made MBE system of base pressure 4×10^{-11} Torr. Si was evaporated at rates of 0.02 nm/s from an *e*-beam evaporator, dopant atoms (Sb and B) from Knudsen cells. Si(100) substrates, of 1000-Ω cm resistivity, and of nominally zero miscut, were chemically cleaned and a protective oxide layer was

grown as the final step.[13] The oxide was desorbed *in situ* at a temperature of 800 °C by deposition of Si,[14] followed by a Si buffer layer. Temperatures during growth were set through the choice of the heater power, which in turn had been calibrated in terms of temperature by laser interferometry.[15] We estimate that the accuracy of this method in the present application is ±20 °C.

Carrier concentration and mobility were determined by the Hall technique in the van der Pauw geometry.[16] A magnetic field of 0.4-T strength was employed. Contact to the buried δ layers was made by highly doped cylindrical regions of a diameter ≈0.5 mm, produced by patterning, deposition of In (*p*-type samples) or Sb (*n*-type samples), and laser annealing. Care was taken to restrict the laser exposure of the sample to the patterned dots. The relationship between the Hall mobility $\mu_{n,p}^H$ and the drift mobility $\mu_{n,p}$, as well as between the Hall concentration n^H, p^H and the carrier concentration n,p, is established via the Hall factor $R_{n,p}^H$. For *n*-type carriers,

$$\mu_n = \frac{\mu_n^H}{R_n^H}, \quad n = n^H R_n^H \tag{1}$$

and, correspondingly, for *p*-type carriers.[17] The Hall factor has been determined for uniformly doped films as $R_n^H = 1.0$ for *n*-type doping, and as $R_p^H = 0.75$ for *p*-type doping.[18] Using these values, excellent agreement between atomic concentration and carrier concentration, i.e., full electrical activation, has been obtained for films grown by LT MBE and doped uniformly in the range of 10^{17}–10^{21} cm^{-3}.[10] We therefore have used the same Hall factors to convert the two-dimensional Hall concentration in a δ layer to a two-dimensional carrier concentration. This approach ignores the effects of confinement and we will discuss this issue further below.

Atomic dopant concentrations were obtained from ion scattering [Rutherford backscattering (RBS)] for Sb, nuclear reaction analysis (NRA) for B, or secondary-ion-mass spectrometry (SIMS) for Sb and B. Typically, 2-MeV He^+ ions, incident about 5° off the surface normal, were employed for RBS. For NRA we made use of the reaction $^{11}B(p,\alpha)^8Be$ for the detection of B with a primary beam energy of 650 keV. Since this reaction detects only the ^{11}B isotope, the measured number of α particles was scaled appropriately with the natural abundance of ^{11}B. The number of backscattered particles or reaction products was converted into an areal density by means of ion-implanted standards of known dose. Samples were continuously rotated around the surface normal to eliminate channeling effects. Sheet concentrations down to ≈5×10^{13} cm^{-2} can be accurately measured in this way. The SIMS analysis was performed with 3-keV Cs^+ ions at a sputter rate of 0.15 nm/s and 2.0-keV O_2^+ ions at a rate of 0.04 nm/s for Sb and B, respectively. In both cases the beam impinged on the sample at an incident angle of 60°. The different techniques agreed within their respective errors.

III. RESULTS

Figure 1 summarizes the results from Hall-effect measurements on single Sb-δ-doped layers; (a) shows the

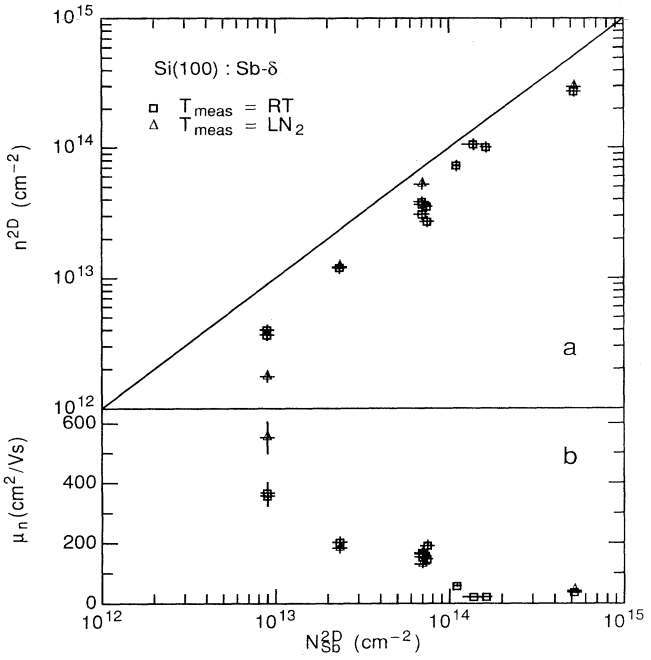

FIG. 1. Sheet concentration (a) and mobility (b) of *n*-type carriers in Sb-δ-doped Si films at room temperature (squares), and liquid-nitrogen temperature (triangles) as a function of atomic sheet concentration. The solid line in (a) corresponds to unity activation. A Hall factor of 1.00 is assumed.

electron concentration and (b) the carrier mobility. The squares represent data taken at room temperature and the triangles were obtained from Hall measurements at liquid-nitrogen temperature. Films were grown at temperatures between 150 and 270 °C with RTA cycles to 600 °C. Typically, the doping spike was buried under 75 nm of Si. The carrier concentration rises linearly with the Sb atomic concentration. However, the ratio between carrier and atomic concentration ("electrically active fraction") is consistently below unity.[19] In fact, it appears to be a constant, independent of concentration, of ≈0.5 and is also independent of temperature in the range between room temperature and liquid-nitrogen temperature [Fig. 1(a)].

Defects such as vacancies can introduce trap levels that bind carriers, thus reducing the active fraction.[20] Such a reduction in the electrical activity of dopants has been observed previously in *uniformly* Sb-doped films grown by solid-phase epitaxy (SPE).[21] Films grown under those conditions are known to contain vacancylike defects with a concentration of the order 10^{18}–10^{19} cm^{-3}.[22,23] They also showed[21] a freeze-out of carriers at liquid-nitrogen temperatures resulting in active fractions of as small as 10^{-2}. Since in this case the volume density of defects is essentially given by the growth method, the active fraction in SPE films is dependent on the doping level: Higher doping concentrations show more activation. However, uniformly doped films grown by LT MBE, under conditions identical to the samples in Fig. 1, always exhibit unity activation[10] and vacancylike defects

are absent (at a sensitivity of 5×10^{15} cm^{-3}).[24] The behavior of the electrical activation of the Sb-δ-doped samples [Fig. 1(a)] is thus not compatible with the existence of defects introduced by the growth method.

Due to the character of a δ function, the peak volume concentration of a dopant in a δ-doped film can reach very high levels, even though the two-dimensional sheet concentration is relatively small. We will next eliminate the possibility that the reduced activation in Fig. 1(a) is due to defects introduced by the spike itself. Such a mechanism would exhibit defect and, thus, trap concentrations proportional to the sheet concentration of the dopant and could thus lead to a deactivation independent of dopant concentration.

For a δ-doped structure, the wave function of a carrier is always wider in the direction along the sample normal than the dopant distribution. Consequently, there is a finite probability that the carriers experience the undoped semiconductor material adjacent to the δ layer. The carrier mobility in a δ-doped film of sheet concentration $N_{A,D}^{2D}$ should therefore be larger than the mobility in the equivalent, uniformly doped film with a dopant concentration $N_{A,D}$. If we demand that the mean distance between dopant atoms in the equivalent, uniformly doped film is the same as in the plane of the dopant sheet in the δ-doped film, then[25]

$$N_{A,D}=(N_{A,D}^{2D})^{3/2}\ . \tag{2}$$

Consider next a δ-doping superlattice, i.e., a train of doping spikes, each spike having a distance d to the next one. As long as d is much larger than the extent of the carrier spilling, the carrier mobility of the doping superlattice (DSL) will be the same as that of a single spike. On the other hand, when d becomes sufficiently small, the wave functions of carriers in neighboring wells will overlap, the characteristic quantum effects of δ doping will vanish, and the system will eventually reach the limit of a uniformly doped semiconductor. The value of d at the crossover is in general not known. A calculation would require the computation of transport properties of single and multiple δ-doped wells; such a computation has not been carried out to our knowledge. Instead we will estimate the order of magnitude of the crossover. A characteristic length scale of the system is the Debye length

$$L_D=\left[\frac{\varepsilon kT}{e^2n}\right]^{1/2}, \tag{3}$$

where ε is the permittivity of the semiconductor, k is Boltzmann's constant, T is the absolute temperature, e is the elementary charge, and n is the volume density of electrons. For $N_{Sb}^{2D}=10^{13}$ cm^{-2} we obtain, with the aid of Eq. (2), $L_D\approx1$ nm. Alternatively, the spatial extent of the ground-state wave (GSW) function has been calculated for a V-shaped potential and an isotropic carrier mass.[26] The result is

$$L_{GSW}=2(\tfrac{7}{5})^{1/2}\left[\frac{4}{9}\frac{\varepsilon\hbar^2}{e^2N_{A,D}^{2D}m^*}\right]^{1/3}, \tag{4}$$

with m^* the effective mass and $\hbar$ Planck's constant divided by 2π, yielding $L_{GSW}\approx2$ nm for $N_{Sb}^{2D}=1\times10^{13}$ cm^{-2} and an effective mass equal to the free-electron mass. This is probably a lower limit since excited subbands that have a wider spatial extent might carry a certain fraction of the total charge. These subbands might also have effective masses smaller than the free-electron mass. Finally, the mean distance between dopant atoms in the sheet [dopant-dopant (DD)], assuming that they occupy only one atomic plane, is given by

$$L_{DD}=[N_{Sb}^{2D}]^{-1/2} \tag{5}$$

which yields $L_{DD}\approx3$ nm for the above example.

We thus except that for periods of the order a few nm the δ-DSL has properties that resemble those of a uniformly doped film much more than those of a film with a single doping spike. The experimental results confirm this expectation. Figure 2 shows the room-temperature electron mobility for films containing 1 and 5–10 doping spikes as a function of the inverse period $1/d$. (A single spike is assigned $1/d=0$.) Each spike has a sheet concentration of $N_{Sb}^{2D}\approx1\times10^{13}$ cm^{-2}. The dashed line represents the mobility of an equivalent, uniformly doped film [Eq. (2), $N_{Sb}=3\times10^{19}$ cm^{-3}].[10] The mobility in the film with one spike is much larger than in the uniformly doped sample, as expected. This is still true, although to a lesser extent, for the DSL's with periods of 20 and 10 nm. The mobility appears to drop exponentially with $1/d$ (solid line) until the superlattice with $d=5$ nm breaks away from the exponential decay, close to the mo-

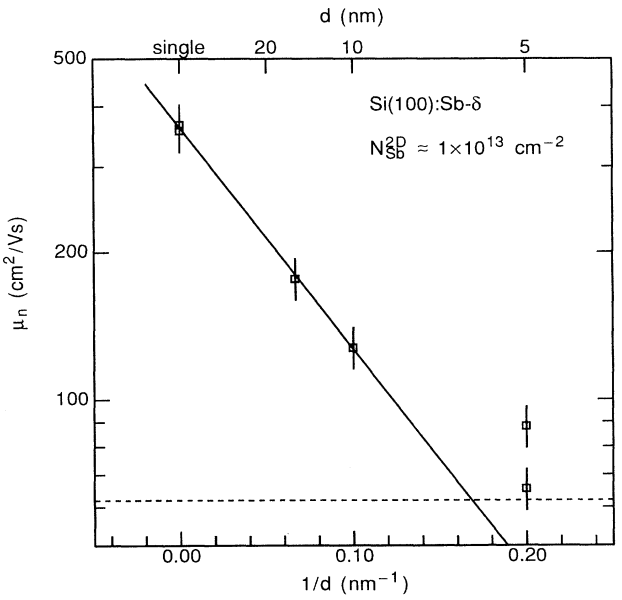

FIG. 2. Room-temperature electron mobility of Si films containing one and 5–10 Sb doping spikes (δ-doping superlattice) as a function of the inverse distance between spikes. (A single spike is assigned $1/d=0$.) Each spike has a sheet concentration of $N_{Sb}^{2D}\approx1\times10^{13}$ cm^{-2}. The dashed line represents the mobility of an equivalent, uniformly doped film [Eq. (2), $N_{Sb}=3\times10^{19}$ cm^{-3}]. The solid line is an exponential fit to the data for $1/d>5$ nm. A Hall factor of 1.00 is assumed.

bility of the equivalent, uniformly doped film. We conclude that for $N_{Sb}=10^{13}$ cm^{-2} the overlap of the electron wave functions is sufficient at $d=5$ nm for the δ-DSL to resemble fairly closely a uniformly doped film, at least as far as the mobility is concerned. In this limit the equivalent volume concentration of a δ-DSL is uniquely given by

$$N_{Sb}=\frac{N_{Sb}^{2D}}{d} . \quad (6)$$

Applying Eq. (6) to a variety of δ-DSL's with $d=5$ nm results in the filled squares in Fig. 3. Excellent agreement of the mobilities is reached between δ-doped and uniformly doped samples (open squares) grown under identical circumstances. Note that at the high concentration end, the mobilities are significantly higher than the values obtained by Masetti, Severi, and Solmi[27] on laser-annealed specimens, which confirms earlier results by Jorke and Kibbel on δ-DSL's with $N_{Sb}^{2D}=6.78\times10^{14}$ cm^{-2}.[28]

The above results on the carrier mobility in δ-DSL's indicate that the material is indistinguishable from uniformly doped samples, for which excellent material quality was established previously.[10] This implies that the observed incomplete electrical activation in films with single doping spikes is not due to growth defects but must be ascribed to an artifact introduced into the Hall measurement by the confinement of the carriers. Since Fig. 2 shows that these effects have been significantly reduced in δ-DSL's with a period of 5 nm, the electrical activity of the dopants in those δ-DSL's should be much closer to 100%. This is indeed observed as can be seen from Fig. 4, which shows the average two-dimensional electron

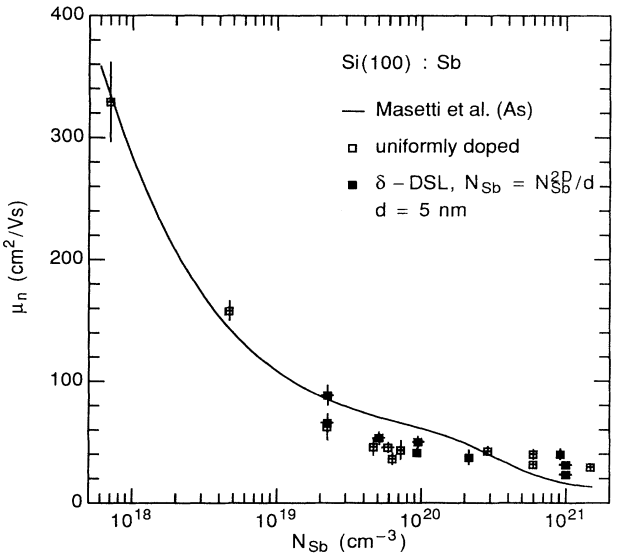

FIG. 3. Room-temperature electron mobility as a function of dopant volume concentration for films doped uniformly with Sb (Ref. 10, open squares), and of Sb-δ-doping superlattices with a distance of $d=5$ nm between spikes. Two-dimensional concentration N_{Sb}^{2D} is converted to volume concentration using Eq. (6). A Hall factor of 1.00 is assumed. The solid line represents the result of Masetti *et al.* (Ref. 27).

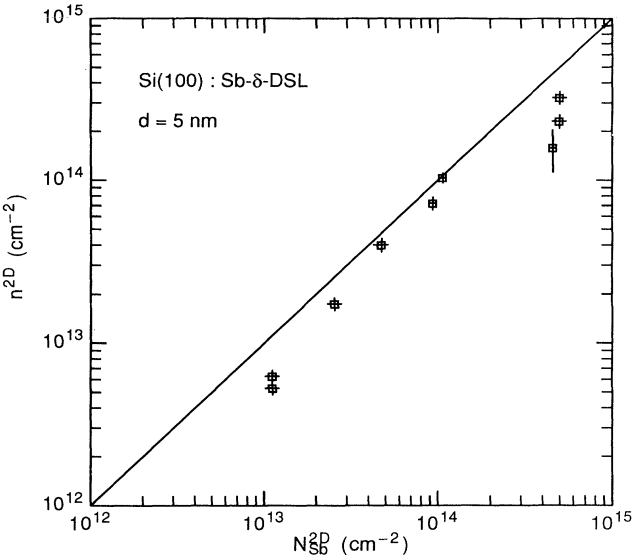

FIG. 4. Average two-dimensional electron concentration per doping spike at room temperature as a function of average dopant sheet concentration per spike for Sb-δ-doping superlattices with a distance of $d=5$ nm between spikes. The solid line represents full electrical activation. A Hall factor of 1.00 is assumed.

concentration per doping spike as a function of the average sheet atomic concentration per spike. We note that depletion due to surface pinning of the Fermi level is small, even for the smallest sheet concentrations. Assuming pinning in midgap, a single δ layer at a depth of 75 nm would be depleted by a sheet charge of $\approx5\times10^{11}$ cm^{-2}. The effect is of the same order of magnitude for the doping superlattices. Although the doping spike closest to the surface might be depleted by $\approx8\times10^{12}$ cm^{-2} for a DSL with period 5 nm, there are typically 10 such spikes in the DSL. Nevertheless, appropriate corrections have been applied to the data in Fig. 4; they were always smaller than 10%. The activity drop visible in Fig. 4 at a concentration of $N_{Sb}^{2D}\approx5\times10^{14}$ cm^{-2} in each spike is due to the deterioration of the crystalline quality observed for those concentrations. The maximum fully active sheet concentration thus appears to be on the order of 10^{14} cm^{-2}; a similar value has also been observed in SPE-grown films.[29] The deviation from 100% activity below 10^{13} cm^{-2} may be due to a freeze-out of carriers. Eisele has reported that at a temperature of 4.2 K a metal-insulator transition takes place in this concentration regime, implying that the system is no longer degenerate.[30] This is also in agreement with the observation in Fig. 1 that only doping spikes with $N_{Sb}^{2D}<1\times10^{13}$ cm^{-2} show a difference in activation between room temperature and liquid-nitrogen temperature.

A full, quantitative understanding of the apparent reduction of electrical activity in films doped with a single spike would require a theory of electrical transport in δ-doped films, including modifications to the Hall coefficient, a self-consistent calculation of the subband structure, and prediction of effective masses. Such a cal-

culation does not exist to our knowledge. We can, however, gain some semiquantitative insight by considering the various subbands and their spatial extent that the carriers occupy in a δ-doped well. To first order we assume that only two subbands are occupied. Then a certain number of carriers, n_1^{2D}, belong to the lowest subband for which the corresponding wave function has an extremum at the position of the dopant sheet. Those carriers experience quite significant scattering and have a fairly low mobility, μ_1. The carriers, of density n_2^{2D}, in the next higher subband have a wave function of odd symmetry, i.e., with a node at the position of the dopant sheet. Consequently, they have a relatively high mobility μ_2. It is straightforward to calculate the Hall effect in such a two-carrier system. Defining by n_{eff}^{2D} that carrier concentration in a one-carrier system that would give the same Hall voltage as the two-carrier system, we obtain

$$\frac{n_{\text{eff}}^{2D}}{n_1^{2D}+n_2^{2D}} = f_{\text{app}} = \frac{(1+\alpha\beta)^2}{(1+\alpha)(1+\alpha\beta^2)} \quad . \tag{7}$$

Here, $\alpha = n_1^{2D}/n_2^{2D}$ and $\beta = \mu_1/\mu_2$. In the context of Eq. (7), the abscissa in Fig. 1 corresponds to n_{eff}^{2D} and $n_1^{2D}+n_2^{2D}$ is the total atomic concentration, N_{Sb}^{2D}. Thus, the right-hand side of Eq. (7) is also equal to the apparent electrical activity f_{app}. Assuming $\alpha=10$ and $\beta=0.1$ gives $f_{\text{app}}=0.33$ from Eq. (7), quite close to the experimental value from Fig. 1, in particular considering the crudeness of the approximations. The apparent electrical activity approaches 1.0 for $\beta \rightarrow 1$, i.e., the Hall measurements would indicate full activation for films where the enhancement of mobility away from the doping plane is small or absent, for example due to growth defects. Such a situation exists for Sb-δ-doped films grown by SPE [see below and Fig. 6(a)] and indeed the Hall activity of these films is unity.[29]

The electrical characterization of single B-δ-doped layers yields results very similar to Sb doping. As Fig. 5(a) shows, the concentration of holes appears significantly

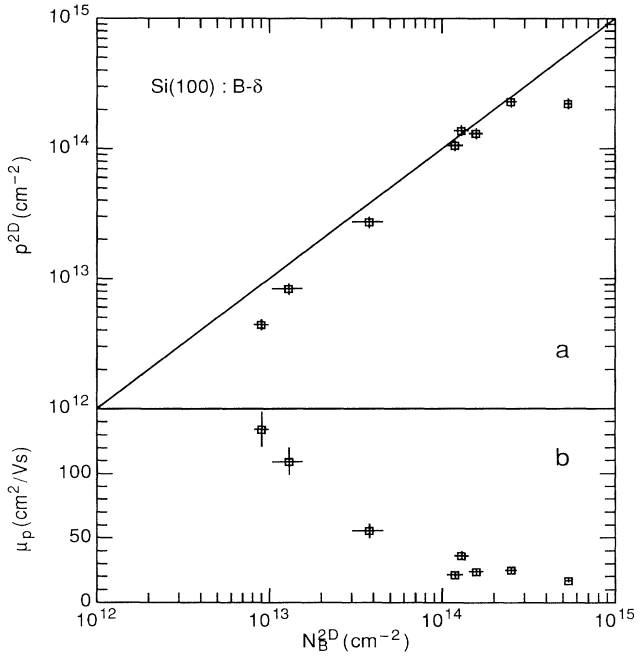

FIG. 5. Sheet concentration (a) and mobility (b) of p-type carriers in B-δ-doped films at room temperature as a function of atomic sheet concentrations (squares). The solid line in (a) corresponds to unity activation. A Hall factor of 0.75 is assumed.

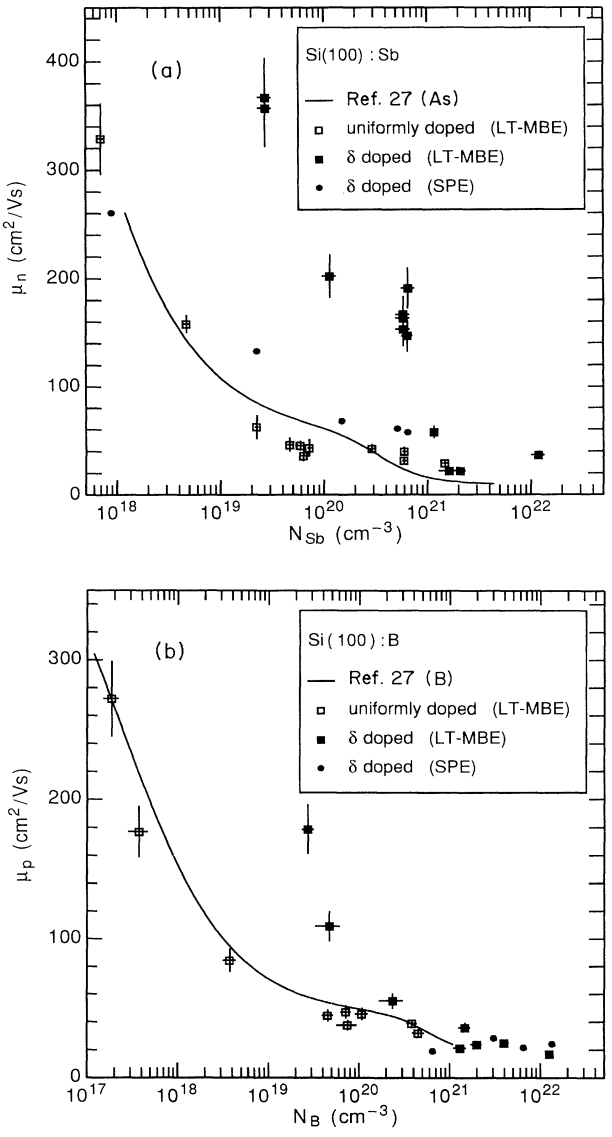

FIG. 6. Room-temperature mobility of electrons (a) and holes (b) in films δ doped with a single spike with Sb (a) and B (b) (filled squares). The two-dimensional concentration of a spike has been converted to a volume concentration using Eq. (2). Included for comparison are the mobilities of uniformly doped films grown by LT MBE (open squares), of δ-doped films grown by SPE [filled circles, from Ref. 29 in (a) and from Ref. 31 in (b)], as well as the results obtained by Masetti *et al.* on uniformly doped bulk samples (solid lines, from Ref. 27). A Hall factor of 1.00 (Sb) and 0.75 (B) is assumed.

below unity with the exception of the data clustered around $N_B^{2D} = 10^{14}$ cm^{-2}. In analogy to the Sb case we ascribe this to confinement of the carriers in the δ-doped well, although the details must certainly differ from Sb doping. We conclude from Fig. 5(a) that the B dopant atoms are completely ionized up to $N_B^{2D} \approx 2 \times 10^{14}$ cm^{-2}, about a factor of 2 more than in the case of Sb. The activation then declines to about 50% at $N_B^{2D} \approx 5 \times 10^{14}$ cm^{-2}.[31] The corresponding hole mobilities are shown in Fig. 5(b).

Figures 6(a) and 6(b) compare the mobilities achievable by δ doping with those of equivalent, uniformly doped films. In each panel we show the mobility as a function of volume concentration, for doping with Sb in (a), with B in (b). Two-dimensional concentrations were converted to volume concentrations using Eq. (2), where applicable. Shown are data from single doping spikes grown by LT MBE (filled squares) and SPE [filled circles, from Ref. 29 for Sb doping in Fig. 6(a), from Ref. 31 for B doping in Fig. 6(b)]. Also shown as solid lines are bulk mobility data up to the maximum reported concentrations,[27] 5×10^{21} cm^{-3} for *n*-type doping (As) and 1.2×10^{21} cm^{-3} for *p*-type doping (B), as well as results from uniformly doped LT MBE grown films (open squares). δ doping obviously has two advantages:[25] (1) Mobilities are significantly higher than in equivalent, uniformly doped films. (2) Up to one order of magnitude, higher volume concentrations are achievable than in uniformly doped films, without deterioration in mobilities. This is particularly evident for Sb doping where the bulk mobilities (solid line) drop to values as low as 10 cm^2/Vs for concentrations beyond 10^{21} cm^{-3}, whereas for δ doping we still measure almost 40 cm^2/Vs at concentrations one order of magnitude higher. In fact, the steep drop in mobility apparent in the bulk curve beyond $\approx 3 \times 10^{20}$ cm^{-3} is completely absent in the LT MBE uniformly or δ-doped films. This could be due to the fact that the samples used for the bulk curve required laser annealing to achieve the high dopant concentration.[27] A similar observation can be made for B: Here, too, the mobility stays approximately constant with concentration in the LT MBE grown, uniformly and δ-doped films beyond a concentration of $\approx 3 \times 10^{20}$ cm^{-3}, whereas the bulk curve starts to drop. Figure 6(a) also demonstrates the comparatively large number of defects present in material grown by SPE: The mobilities in Sb-δ-doped films grown by SPE are much smaller than in the films grown by LT MBE. This effect becomes masked at concentrations beyond $\approx 5 \times 10^{20}$ cm^{-3} (corresponding to $N_{Sb}^{2D} = 5 \times 10^{13}$ cm^{-2}), as the B data illustrate.

IV. CONCLUSION

The electrical characteristics of Si films grown by LT MBE and doped with single or multiple δ-like doping profiles have been investigated. The apparent reduction in electrical activity is *not* due to some form of imperfection of the grown material. Comparison of singly δ-doped layers with δ-doping superlattices clearly shows that the apparent reduction in electrical activity must be due to the effects of confinement of the carriers in the potential well of the doping spike and explicitly confirms previous suggestions.[30] Thus, care must be taken when deducing free-carrier concentrations in δ-doped films from Hall measurements. The reduced activity and the general trend of the observations can be described semiquantitatively by considering a two-carrier system. It is, however, clear that a full quantitative treatment requires a self-consistent calculation of electrical transport in δ-doped films that includes the effects of direct changes in the electronic structure of the system, such as changes in carrier effective mass, and changes to the transport properties, for example a variation in the Hall factor. While Hall factors have been theoretically investigated for uniform doping, and are found to be dependent on concentration,[18] no such investigation is known to us for a δ-doped system.

The effect of the confinement can be reduced in δ-doping superlattices, provided the distance between doping spikes is sufficiently small. For $N_{Sb}^{2D} = 10^{13}$ cm^{-2}, the mobility in a δ-doped superlattice drops exponentially as a function of inverse distance until at a spacing of about 5 nm deviations occur away from the exponential drop, and a mobility close to that of an equivalent, uniformly doped film is reached.

δ doping is able to yield material with dopant volume concentrations beyond 10^{22} cm^{-3}, yet with significant mobilities. The known bulk curves have been extended in this way. Mobilities in δ-doped films exhibit values significantly larger than these bulk curves, i.e., the extreme peak volume concentrations present in the δ spike do not degrade the material quality.

ACKNOWLEDGMENTS

We acknowledge helpful discussions with V. M. Donnelly, D. J. Eaglesham, L. C. Feldman, D. R. Hamann, D. Monroe, J. M. Poate, and E. F. Schubert. SIMS analysis by H. S. Luftman and substrate preparation by T. Boone are greatly appreciated.

[1]T. P. Pearsall, J. Bevk, L. C. Feldman, A. Ourmazd, J. M. Bonar, J. P. Mannaerts, and B. A. Davidson, Appl. Phys. Lett. **50**, 760 (1987).

[2]Y. J. Mii, Y. H. Xie, E. A. Fitzgerald, D. Monroe, F. A. Thiel, and B. E. Weir, Appl. Phys. Lett. **59**, 1611 (1991).

[3]D. Monroe, Y. H. Xie, E. A. Fitzgerald, and P. J. Silverman, Phys. Rev. B **46**, 7935 (1992).

[4]E. F. Schubert and K. Ploog, Jpn. J. Appl. Phys. Lett. **24**, L608 (1985).

[5]For a review see H.-J. Gossmann and E. F. Schubert, CRC Crit. Rev. Solid State Mater. Sci. (to be published).

[6]H. P. Zeindl, T. Wegehaupt, I. Eisele, H. Oppolzer, H. Reisinger, G. Tempel, and F. Koch, Appl. Phys. Lett. **50**, 1164 (1987).

[7]H. Jorke, H. Kibbel, F. Schäffler, A. Casel, H.-J. Herzog, and E. Kasper, Appl. Phys. Lett. **54**, 819 (1989).

[8]M. W. Denhoff, T. E. Jackman, J. P. McCaffrey, J. A. Jackman, W. N. Lennard, and G. Massoumi, Appl. Phys. Lett. **54**,

1332 (1989).
[9]N. L. Mattey, M. G. Dowsett, E. H. C. Parker, T. E. Whall, S. Taylor, and J. F. Zhang, Appl. Phys. Lett. **57**, 1648 (1990).
[10]H.-J. Gossmann, F. C. Unterwald, and H. S. Luftman, J. Appl. Phys. (to be published).
[11]D. J. Eaglesham, H.-J. Gossmann, and M. Cerullo, Phys. Rev. Lett. **65**, 1227 (1990).
[12]H. Jorke, H.-J. Herzog, and H. Kibbel, Phys. Rev. B **40**, 2005 (1989).
[13]A. Ishizaka and Y. Shiraki, J. Electrochem. Soc. **133**, 666 (1986).
[14]M. Tabe, Jpn. J. Appl. Phys. **21**, 534 (1982).
[15]V. M. Donnelly and J. A. McCaulley, J. Vac. Sci. Technol. A **8**, 84 (1990).
[16]L. J. van der Pauw, Philips Res. Rep. **13**, 1 (1958).
[17]S. M. Sze, *Physics of Semiconductor Devices* (Wiley, New York, 1981).
[18]J. F. Lin, S. S. Li, L. C. Linares, and K. W. Teng, Solid State Electron. **24**, 827 (1981).
[19]We can exclude the possibility that the observed reduction in carrier concentration is an artifact of the Hall measurement produced by a second carrier type, for example, from the substrate. The substrate for the *n*-type δ layers is *p* doped to a resistivity of 1000 Ω cm; if, despite the isolation via a *p-n* junction, carriers from the substrate would contribute to the Hall voltage of the film, they would tend to reduce the observed Hall voltage, thus increasing the apparent carrier concentration, which is inversely proportional to the Hall voltage, contrary to the actual experimental observation.
[20]B. N. Mukashev, L. G. Kolodin, K. H. Nussupov, A. V. Spitsyn, and V. S. Vavilov, Rad. Eff. **46**, 79 (1980).
[21]A. Casel, H. Kibbel, and F. Schäffler, Thin Solid Films **183**, 351 (1990).
[22]H. Schut, A. van Veen, G. F. A. van de Walle, and A. A. van Gorkum, J. Appl. Phys. **70**, 3003 (1991).
[23]P. Asoka-Kumar, H.-J. Gossmann, T. C. Leung, V. Talyanski, B. Nielsen, K. G. Lynn, F. C. Unterwald, and L. C. Feldman (unpublished).
[24]H.-J. Gossmann, P. Asoka-Kumar, T. C. Leung, B. Nielsen, K. G. Lynn, F. C. Unterwald, and L. C. Feldman, Appl. Phys. Lett. **61**, 540 (1992).
[25]E. F. Schubert, J. E. Cunningham, and W. T. Tsang, Solid State Commun. **63**, 591 (1987).
[26]E. F. Schubert, R. F. Kopf, J. M. Kuo, H. S. Luftman, and P. A. Garbinski, Appl. Phys. Lett. **57**, 497 (1990).
[27]G. Masetti, M. Severi, and S. Solmi, IEEE Trans. Electron Devices **ED-30**, 764 (1983).
[28]H. Jorke and H. Kibbel, Thin Solid Films **183**, 323 (1989).
[29]A. A. van Gorkum, K. Nakagawa, and Y. Shiraki, J. Appl. Phys. **65**, 2485 (1989).
[30]I. Eisele, Appl. Surf. Sci. **36**, 39 (1989).
[31]R. L. Headrick, B. E. Weir, A. F. J. Levi, D. J. Eaglesham, and L. C. Feldman, Appl. Phys. Lett. **57**, 2779 (1990).